

# B-physics anomalies: The bridge between R-parity violating Supersymmetry and flavoured Dark Matter

Sokratis Trifinopoulos<sup>\*1</sup>

<sup>1</sup>*Physik-Institut, Universität Zürich, CH-8057 Zürich, Switzerland*

## Abstract

In recent years, significant experimental indications that point towards Lepton Flavour Universality violating effects in B-decays, involving  $b \rightarrow c\tau\nu$  and  $b \rightarrow s\ell^+\ell^-$  have been accumulated. A possible New Physics explanation can be sought within the framework of R-parity violating Supersymmetry, which contains the necessary ingredients to explain the anomalies via both leptoquark, tree-level exchange and one-loop diagrams involving purely leptonic interactions. In addition, an approximate  $U(2)^2$  flavour symmetry, that respects gauge coupling unification, successfully controls the strength of these interactions. Nevertheless strong constraints from leptonic processes and  $Z$  boson decays exclude most of the relevant parameter space at the  $2\sigma$  level. Moreover, R-parity violation deprives Supersymmetry of its Dark Matter candidates. Motivated by these deficiencies, we introduce a new gauge singlet superfield, charged under the flavour symmetry and show that its third-generation, scalar component may participate in loop diagrams that alleviate the above-mentioned tensions, while at the same time reproduce the observed relic abundance. Remarkably, we obtain a very effective solution to both anomalies that is also fully consistent with the rich Flavour and Dark Matter phenomenology. Finally, we assess the prospect to probe the model at future experiments.

---

<sup>\*</sup>trifinos@physik.uzh.ch

# Contents

<b>1</b>	<b>Introduction</b>	<b>3</b>
<b>2</b>	<b>Model</b>	<b>4</b>
2.1	R-parity violating interactions . . . . .	4
2.2	Supersymmetric flavoured Dark Matter . . . . .	5
2.3	Flavour Structure . . . . .	6
<b>3</b>	<b>Observables</b>	<b>7</b>
3.1	B mesons . . . . .	7
3.2	$Z \rightarrow \ell\bar{\ell}'$ coupling and $\tau$ decays . . . . .	9
3.3	Relic abundance and Dark Matter direct detection . . . . .	11
3.4	Collider searches . . . . .	12
<b>4</b>	<b>Phenomenological Analysis</b>	<b>12</b>
<b>5</b>	<b>Conclusions</b>	<b>14</b>

# 1 Introduction

Testing the limits of the Standard Model (SM) by examining processes that might not respect Lepton Flavor Universality (LFU) is one of the most prominent endeavors to discover New Physics (NP) pursued at the LHC and several other experiments. Intriguingly, recent data exhibit anomalies in rare B-meson LFU violating decays, as encoded by the ratios:

$$R_{K^{(*)}} = \frac{\mathcal{B}(B \rightarrow K^{(*)}\mu\bar{\mu})}{\mathcal{B}(B \rightarrow K^{(*)}e\bar{e})}, \quad \text{and} \quad R_{D^{(*)}} = \frac{\mathcal{B}(B \rightarrow D^{(*)}\tau\bar{\nu})}{\mathcal{B}(B \rightarrow D^{(*)}\ell\bar{\nu})}; \quad \ell = e, \mu \quad (1)$$

which are almost free from theoretical uncertainties in hadronic matrix elements.  $R_{D^{(*)}}$  concerns an enhancement of the charged-current interaction  $b \rightarrow c\tau\nu$  [1–5] with respect to the tree-level induced SM amplitude [6] [7], whereas  $R_{K^{(*)}}$  a deficit in neutral-current transition involving  $b \rightarrow s\ell^+\ell^-$  [8] [9] at one-loop level [10]. They independently differ by approximately  $3 - 4\sigma$  from their respective SM predictions and along with reported indications towards LFU violation in less theoretically-clean observables, e.g. the angular observable  $P'_5$  in the  $B \rightarrow K^*\mu\bar{\mu}$  decay [11–13] and the  $R_{J/\Psi}$  ratio [14, 15], constitute a consistent pattern of deviations that has motivated several attempts for a simultaneous explanation [16–60]. Nevertheless, the theoretical challenge to devise an ultraviolet (UV) complete model that accommodates all other low-energy observables, has proven to be notoriously difficult and to the best of our knowledge, there have only been a handful of proposals in the bibliography so far [36, 39, 40, 42, 44, 47, 58].

Considering that the charged-current anomaly involves the tau and both of them the bottom, NP scenarios in which the third-generation SM fermions play a special role are favoured. Furthermore, model-independent analyses suggest that  $R_{K^{(*)}}$  can be resolved by singly modifying the Wilson Coefficient (WC) of the semi-leptonic di-muon vector and axial operators, i.e.  $C_9^\mu$  and  $C_{10}^\mu$  [61–63]. In light of these observations, the potential of R-parity violating (RPV) Supersymmetry (SUSY) to provide a comprehensive solution has been studied [52–59]. The Minimal Supersymmetric Standard Model (MSSM) particle content contains two third-generation, scalar particles, namely the right-handed sbottom  $\tilde{b}_R$  and stau  $\tilde{\tau}_R$ , which in most models of spontaneous SUSY breaking are predicted to be significantly lighter than the first and second generations of superpartners at the electroweak scale [64]. If RPV interactions are turned on,  $\tilde{b}_R$  has the right quantum numbers to mediate the required, large NP effects on  $R_{D^{(*)}}$  at tree-level, while according to the novel result of [58],  $\tilde{\tau}_R$  and  $\tilde{b}_R$  can enter a box diagram, which generates a negative contribution to  $C_9^\mu$ . Additionally, inspired by the corresponding Effective Field Theory (EFT) studies [18, 22, 31, 32], it was shown that an approximate  $U(2)^2$  flavour symmetry<sup>1</sup>, acting only on the first two generations, naturally suppresses the RPV couplings within the experimental bounds and still allows for an improvement over the SM fit. However the possibility to completely alleviate the tensions in the ratios 1 and especially in  $R_{K^{(*)}}$  is severely limited by the strict bounds on  $Z$  boson decay to leptons and tree-level, Lepton Flavor Violating (LFV)  $\tau$  decays.

The RPV setup preserves all the attractive features of SUSY, but one, namely the Lightest Supersymmetric Particle (LSP) acting as Dark Matter (DM) candidate, because RPV interactions render it unstable. Therefore, we are compelled to speculate on the existence of new

---

<sup>1</sup>Historically, the  $U(2)$  flavour symmetries have strong ties with SUSY as their initial proposal intended to solve the ‘flavour problem’ of the MSSM [65] [66]. This is also true for the WIMP paradigm, since the LSP in R-parity conserving SUSY has been cherished as the prototype of a WIMP particle and a point of reference for direct searches.

particles and the simplest, most popular example is that of a weakly interacting massive particle (WIMP)<sup>2</sup>, which is thermally produced in the early universe. Among the numerous WIMP models, those that assume a direct DM coupling to specific SM fermions and hence furnish distinctive collider signatures, are of particular interest. As with the case of RPV interactions, we would like to justify the apparent suppression of DM interactions with the first SM generation, which is most relevant to direct detection experiments. Consequently, we focus on the subclass of models, that explains from a flavour symmetry rationale the preference of DM to couple predominantly to particular flavours of either quark [67–79] or leptons [80–90], usually in Minimal Flavour Violation (MFV) -type scenarios. Moreover, supersymmetric flavored DM models exhibit an even more restricted structure due to the holomorphicity of the superpotential [71].

As long as the nature of DM remains a mystery, it is important to investigate any possible connection with other anomalous observations. To this end, there have been attempts to link mostly the  $R_{K^{(*)}}$  discrepancy with DM [91–112]. In the current work, we address both anomalies in a supersymmetric framework related to a flavoured hidden sector. The new particle content is economical, simply consisting of a gauge singlet, flavour multiplet and a  $SU(2)_L$  doublet, flavour singlet, chiral superfield, that acts as the mediator of a DM-lepton interaction. In analogy to the assumed MSSM mass spectrum, the third-generation scalar contained in the multiplet is taken to be the lightest component and thus the DM candidate. We revisit the  $U(2)^2$  flavour symmetry that controls the strength of both DM and RPV interactions, so that it is compatible with Grand Unification Theories (GUTs). By virtue of the spin and unsuppressed coupling of the DM particle to the  $\tau_L$ , contributions are generated in one-loop diagrams involving purely leptonic interactions that interfere destructively with the ones generated by the RPV interactions. By exploring the interplay between the rich flavour and DM phenomenology, we determine whether it is possible to invoke an appropriate cancellation mechanism and at the same time reproduce the correct relic abundance for a natural choice of parameters. The performance of the overall fit is subsequently evaluated. Finally, we briefly discuss the implications for future experiments.

## 2 Model

### 2.1 R-parity violating interactions

Let us first review the R-parity odd and gauge-invariant superpotential, composed exclusively of MSSM quark and lepton superfields [113],

$$W_{\text{RPV}} = \frac{1}{2} \lambda_{ijk} L_i L_j E_k^c + \lambda'_{ijk} L_i Q_j D_k^c + \frac{1}{2} \lambda''_{ijk} U_i^c U_j^c D_k^c, \quad (2)$$

where there is a summation over the flavour indices  $i, j, k = 1, 2, 3$ , and summation over gauge indices is understood.

The traditional motivation for R-parity is that it forbids the baryon-number braking  $\lambda''$  couplings and thus ensures proton stability, but this argument is no longer substantial. Notwithstanding, if the MSSM is an effective theory [114], higher-dimensional operators could also induce rapid proton decay and one should rely on different mechanisms, e.g. MFV-type flavour symmetries, to mitigate the effect [115] [116]. Here, it is also worth mentioning that since direct

---

<sup>2</sup>See footnote 1.

searches at LHC have been unfruitful so far [117], a ‘vanilla’ MSSM scenario with 10% fine-tuning is ruled out [118]. The exploration of non-minimal realisations of SUSY with reduced missing energy signatures, such as RPV SUSY, as viable model building directions is therefore prominent [119–121].

As already noted in the introduction, we may treat only the third generation as effectively supersymmetrized, a premise that is also supported by general bottom-up approaches [114] [122]. The low-energy spectrum can be further simplified by assuming that the left-handed superpartners are also heavier by an order of magnitude. The trilinear terms associated with the  $\lambda$  and  $\lambda'$  couplings that are relevant to our discussion and expanded in standard four-component Dirac notation, are then,

$$\mathcal{L}_\lambda = -\frac{1}{2}\lambda_{ij3}(\tilde{\tau}_R^*\bar{\nu}_{Ri}^c\ell_{Lj} - (i \leftrightarrow j)) + \text{h.c.} \quad (3)$$

$$\mathcal{L}_{\lambda'} = -\lambda'_{ij3}\left(\tilde{b}_R^*\bar{\nu}_{Ri}^cd_{Lj} - \tilde{b}_R^*\bar{\ell}_{Ri}^cu_{Lj}\right) + \text{h.c.} \quad (4)$$

For the sake of simplicity, we shall assume that the couplings are real numbers.

## 2.2 Supersymmetric flavoured Dark Matter

	$SU(3)_c$	$SU(2)_L$	$U(1)_Y$	$U(2)_T$	$U(2)_{\bar{F}}$
$(Q_1, Q_2)$	<b>3</b>	<b>2</b>	1/6	<b>2</b>	<b>1</b>
$Q_3$	<b>3</b>	<b>2</b>	1/6	<b>1</b>	<b>1</b>
$(U_1^c, U_2^c)$	<b>3</b>	<b>1</b>	-2/3	<b>2</b>	<b>1</b>
$U_3^c$	<b>3</b>	<b>1</b>	-2/3	<b>1</b>	<b>1</b>
$(D_1^c, D_2^c)$	<b>3</b>	<b>1</b>	1/3	<b>1</b>	<b>2</b>
$D_3^c$	<b>3</b>	<b>1</b>	1/3	<b>1</b>	<b>1</b>
$(L_1, L_2)$	<b>1</b>	<b>2</b>	-1/2	<b>1</b>	<b>2</b>
$L_3$	<b>1</b>	<b>2</b>	-1/2	<b>1</b>	<b>1</b>
$(E_1^c, E_2^c)$	<b>1</b>	<b>1</b>	-1	<b>2</b>	<b>1</b>
$E_3^c$	<b>1</b>	<b>1</b>	-1	<b>1</b>	<b>1</b>
$(X_1, X_2)$	<b>1</b>	<b>1</b>	0	<b>1</b>	<b>2</b>
$X_3$	<b>1</b>	<b>1</b>	0	<b>1</b>	<b>1</b>
$Y$	<b>1</b>	<b>2</b>	-1/2	<b>1</b>	<b>1</b>

Table 1: Quark, Lepton and Dark Matter chiral superfields and their gauge and flavour quantum numbers.

We extend the matter content of the MSSM introducing a vector-like DM flavour multiplet  $X, \bar{X}$  and a vector-like mediator  $Y, \bar{Y}$ . The requirement that  $X$  is a gauge singlet and couples to the left-handed leptons fixes the quantum numbers of the new superfields as shown in Table 1. It follows, that the mediator is charged under the MSSM gauge group. The most general superpotential relevant to the new superfields can be expressed as,

$$W_{\text{DM}} = \hat{M}_X X \bar{X} + \hat{M}_Y Y \bar{Y} + \hat{\lambda}_{ij} X_i Y L_j, \quad (5)$$

where  $i, j = 1, 2, 3$  denote again flavour indices.

A crucial difference between generic models of flavoured DM and the supersymmetric setup is that the superpotential needs to be holomorphic. It is due to this property, that the  $\hat{\lambda}$ -term is the only Yukawa interaction that we are permitted to include at renormalizable level. For instance, the so-called Higgs Portal of scalar DM models, i.e. a scalar cubic interaction between  $X$  and the Higgs, is absent. This is an important point, given the fact that such an interaction is strongly constrained by direct detection searches [123] and in generic scalar DM models one must set the coupling arbitrarily to zero.

As far as the mass terms are concerned, they are obviously non-holomorphic and indeed their origin lies in terms of the Kähler potential that can be associated with the soft SUSY breaking scale in a way analogous to the Giudice-Masiero mechanism [124]. In synergy with non-canonical kinetic terms, which are expanded as functions of flavour spurions, a large mass splitting between  $X_3$  and the nearly degenerate  $X_1$  and  $X_2$  can be obtained [71]. In addition, soft-breaking terms in the hidden sector produce an additional mass splitting between the scalar and fermionic components. As a result, the scalar component  $\chi$  of  $X_3$  can be the lightest DM state and together with the fermion component  $\psi$  of  $Y$ , they build the term

$$\mathcal{L}_{\hat{\lambda}} = \hat{\lambda}_{3j} \bar{\ell}_{Lj} \chi \psi + \text{h.c.}, \quad (6)$$

which is the interaction term relevant to low-energy phenomenology.

Regarding the DM stabilization, we notice that because  $X$  is leptophilic and the flavour-breaking sources are not MFV-type, we cannot apply the mechanism of the residual  $Z_3$  symmetry that exists for quark-flavoured DM [69, 76]. One can envision alternatives in an extended hidden sector with its own gauge symmetries, but this discussion is beyond the scope of the current paper. We shall simply assume a  $Z_2$  symmetry, under which  $X$  and  $Y$  are odd and their direct decay to SM particles is forbidden.

### 2.3 Flavour Structure

Following EFT approaches [18, 22, 31, 32], a non-abelian flavour symmetry  $U(2)_q \times U(2)_\ell$  was employed in Ref. [58]. Under the assumption that it is spontaneously broken by the vacuum expectation values (VEVs) of two different sets of flavon fields, one quark- and one lepton-flavoured, the observed fermion mass hierarchy and the phenomenologically viable hierarchy of RPV couplings is reproduced [125]. Nevertheless, such a breaking pattern is against the idea of gauge coupling unification<sup>3</sup>. It is thus suitable to adopt a different version of the  $U(2)^2$  flavour symmetry group that commutes with  $SU(5)$ , which is contained in all GUT groups. In terms of the the  $\mathbf{10}_i(T_i) \oplus \bar{\mathbf{5}}_i(\bar{F}_i)$  ( $i = 1, 2, 3$ ) representations of  $SU(5)$ , the plausible choice is the flavour symmetry  $U(2)_T \times U(2)_{\bar{F}}$  [126], under which the matter superfields transform as,

$$\mathbf{T} = (T_1, T_2) \sim (\mathbf{2}, \mathbf{1}), \quad T_3 \sim (\mathbf{1}, \mathbf{1}), \quad \bar{\mathbf{F}} = (\bar{F}_1, \bar{F}_2) \sim (\mathbf{2}, \mathbf{1}), \quad \bar{F}_3 \sim (\mathbf{1}, \mathbf{1}). \quad (7)$$

In Table 1, the same transformation properties are expressed in terms of the MSSM superfields. In a minimal fashion, we assign  $U(2)_{\bar{F}}$  charge to the doublet consisting of the first two generations of  $X$ , but in an extended scenario, where the mass splitting between the components of

---

<sup>3</sup>Note that the beyond-the-MSSM elements postulated in this work do not spoil gauge coupling unification. In particular, RPV interactions even in the limit where the first two generations are decoupled, do not alter the RG evolution up to a shift of the unified coupling value [56] and if the SM-charged mediator  $Y$  is embedded in a complete GUT multiplet, e.g. for  $SU(5)$  in an antifundamental  $\bar{\mathbf{5}}$ , then unification is still preserved.

$X$  is smaller, it may be reasonable to postulate a separate flavour symmetry  $U(2)_X$  in analogy to the Refs [76] and [89].

The  $SU(5)$ -invariant Yukawa Lagrangian,

$$\begin{aligned}\mathcal{L}_Y = & y_t T_3 T_3 H_5 + y_t x_t \mathbf{T} \mathbf{V}_T T_3 H_5 + \mathbf{T} \Delta_T \mathbf{T} H_5 + y_b T_3 \bar{F}_3 H_5 \\ & + y_b x_b \mathbf{T} \mathbf{V}_T \bar{F}_3 H_{\bar{5}} + \mathbf{T} \Delta_{T \times \bar{F}} \bar{\mathbf{F}} H_{\bar{5}},\end{aligned}\quad (8)$$

is also kept flavour-invariant by ascribing to the spurions  $\mathbf{V}_T$ ,  $\Delta_T$  and  $\Delta_{T \times \bar{F}}$  the appropriate transformation properties. The masses and the mixings in the low-energy limit are then qualitatively understood<sup>4</sup> with the following alignment of the spurions in flavour space,

$$\mathbf{V}_T = (0 \ \epsilon)^T, \quad \Delta_T = \begin{pmatrix} 0 & \epsilon' \\ -\epsilon' & \epsilon\rho \end{pmatrix}, \quad \Delta_{T \times \bar{F}} = \begin{pmatrix} 0 & \epsilon' \\ -\epsilon' & \epsilon \end{pmatrix} \quad (9)$$

the symmetry breaking parameters  $\epsilon \approx 0.025$  and  $\epsilon' \approx 0.006$  and the higher order correcting parameter  $\rho \approx 0.02$  [128].

In contrast to MFV with holomorphic Yukawa spurions [116], all trilinear terms in the superpotential 2 and 5 can be converted to holomorphic flavour singlets by appropriately contracting the matter superfields with the above spurions and an additional spurion  $\mathbf{V}_{\bar{F}}$  transforming as  $(\bar{\mathbf{2}}, \mathbf{1})$ . In retrospect, we know that the  $b \rightarrow s\ell^+\ell^-$  anomalies imply a sizeable coupling  $\lambda_{323}$ , possibly of order  $\mathcal{O}(1)$ . Since there is no term of the form  $\bar{\mathbf{F}} \mathbf{V}_{\bar{F}} \bar{F}_3$  in Eq. 8, we have the freedom to write:  $\mathbf{V}_{\bar{F}} = (0 \ \epsilon_{\bar{F}})^T$  with  $\epsilon_{\bar{F}} \approx 1$ . As a result of this symmetry and symmetry-breaking ansatz, we achieve a flavour structure similar to the one proposed in [58], but this time with a more appealing theoretical justification. Last but not least, a thorough study of the connection between the RPV trilinear and the Yukawa couplings in the context of  $SU(5)$  may reveal the conditions under which the relation  $\lambda_{323} \approx \lambda'_{233} \approx \lambda'_{333}$  is a prediction of the model [129].

### 3 Observables

In this Section, we analyse the impact of the RPV and DM interactions on low-energy observables. We focus on the processes that receive NP contributions dependent on the unsuppressed couplings  $\lambda_{323}$ ,  $\lambda'_{233}$ ,  $\lambda'_{333}$ ,  $\hat{\lambda}_{32}$  and  $\hat{\lambda}_{33}$  or at least by the  $\epsilon$ -suppressed couplings  $\lambda'_{223}$  and  $\lambda'_{323}$ . The relevant experimental values and upper bounds are listed in Table 2.

#### 3.1 B mesons

The processes that involve the B meson are affected solely by RPV interactions. To begin with, one can build four-fermion, semi-leptonic operators that generate contributions to B meson decays from the trilinear terms in 4 by a tree-level sbottom exchange. Working in the mass eigenbasis for the down-type quarks, the effective Lagrangians read,

$$\mathcal{L}(b \rightarrow c\ell\bar{\nu}_\ell) = -\frac{4G_F}{\sqrt{2}} V_{cb} (\delta_{ii'} + \Delta_{ii'}^c) \bar{\ell}_L^{i'} \gamma^\mu \nu_L^i \bar{c}_L \gamma_\mu b_L, \quad (10)$$

$$\mathcal{L}(b \rightarrow s\nu\bar{\nu}) = -\frac{4G_F}{\sqrt{2}} \frac{\alpha_{\text{em}}}{2\pi s_W^2} X_t V_{ts}^* V_{tb} (\delta_{ii'} + X_{ii'}^s) \bar{\nu}_L^{i'} \gamma^\mu \nu_L^i \bar{s}_L \gamma_\mu b_L, \quad (11)$$

---

<sup>4</sup>The correct Yukawa matrices are derived only after further refinement of Eq. 8 by including a term of the form  $\mathbf{T} \Delta'_{T \times \bar{F}} \bar{\mathbf{F}} H_{\bar{4}5}$  that generates different  $\mu - s$  and  $e - d$  masses and leads to the Georgi-Jarlskog mass relation [127].

observable	experimental value
$r_{D^{(*)}}$	$1.139 \pm 0.053^5$
$\delta C_9^\mu = -\delta C_{10}^\mu$	$-0.53 \pm 0.09$ [63]
$R_{B \rightarrow K^{(*)}\nu\bar{\nu}}$	$< 5.2$ [31]
$C_{B_s}$	$1.070 \pm 0.088$ [130]
$\Delta M_{B_d}$	$(3.327 \pm 0.013) \times 10^{-13}$ GeV [131]
$\frac{a_\tau}{a_e}$	$1.0019 \pm 0.0015$ [132]
$R_\tau^{\tau/\mu}$	$1.0022 \pm 0.0030$ [133]
$\mathcal{B}(\tau \rightarrow \mu\mu\bar{\mu})$	$< 2.1 \times 10^{-8}$ [132]
$\mathcal{B}(\tau \rightarrow \mu\gamma)$	$< 4.4 \times 10^{-8}$ [132]

Table 2: Experimental values and SM predictions for the observables used in the numerical analysis.

where

$$\Delta_{ii'}^c = \sum_{j'=s,b} \frac{\sqrt{2}}{4G_F} \frac{\lambda'_{i33}\lambda'_{i'j'3}}{2m_{\tilde{b}_R}^2} \frac{V_{cj'}}{V_{cb}}, \quad X_{ii'}^s = -\frac{\pi s_W^2}{\sqrt{2}G_F\alpha_{\text{em}}X_t V_{ts}^* V_{tb}} \left( \frac{\lambda'_{i33}\lambda'_{i'23}}{2m_{\tilde{b}_R}^2} \right), \quad (12)$$

and  $X_t = 1.469 \pm 0.017$  is a SM loop function [134]. The processes of interest are the charged-current  $b \rightarrow c\tau\nu$  anomaly and the  $B \rightarrow K^{(*)}\nu\bar{\nu}$  decay. The NP effects are probed by the ratios [54]:

$$r_{D^{(*)}} = \frac{R_{D^{(*)}}}{R_{D^{(*)}}^{\text{SM}}} = \frac{|1 + \Delta_{33}^c|^2 + |\Delta_{23}^c|^2}{\frac{1}{2}(1 + |\Delta_{22}^c|^2 + |\Delta_{32}^c|^2)} \quad \text{and} \quad (13)$$

$$R_{B \rightarrow K^{(*)}\nu\bar{\nu}} = \frac{\mathcal{B}(B \rightarrow K^{(*)}\nu\bar{\nu})}{\mathcal{B}(B \rightarrow K^{(*)}\nu\bar{\nu})_{\text{SM}}} = \sum_{i=\mu,\tau} \frac{1}{3} |1 + X_{ii}^s|^2 + \sum_{i \neq i'} \frac{1}{3} |X_{ii'}^s|^2. \quad (14)$$

The reported enhancement of  $r_{D^{(*)}}$  favours large (resp. small) values for the coupling  $\lambda'_{333}$  (resp.  $\lambda'_{233}$ ) and the coupling combination  $\lambda'_{323}\lambda'_{333}$  (resp.  $\lambda'_{223}\lambda'_{233}$ ), while  $R_{B \rightarrow K^{(*)}\nu\bar{\nu}}$  sets a strong upper bound on the sum of the same coupling combinations.

At one-loop level, contributions to the neutral-current  $b \rightarrow s\ell\bar{\ell}$  anomaly are generated. The effective Lagrangian is parametrized as,

$$\mathcal{L}(b \rightarrow s\ell\bar{\ell}) = \frac{4G_F}{\sqrt{2}} \frac{\alpha_{\text{em}}}{4\pi} V_{tb} V_{tb}^* \left[ (C_9^\ell + \delta C_9^\ell) \bar{\ell}^{i'} \gamma^\mu \ell^i \bar{s}_L \gamma_\mu b_L + (C_{10}^\ell + \delta C_{10}^\ell) \bar{\ell}^{i'} \gamma^\mu \gamma_5 \ell^i \bar{s}_L \gamma_\mu b_L \right], \quad (15)$$

---

<sup>5</sup>The value for  $r_{D^{(*)}}$  is calculated according to Eq. 13 as the fraction of the weighted average of the  $R_D$  and  $R_{D^*}$  most recent experimental world average [5] over the weighted average of the  $R_D^{\text{SM}}$  and  $R_{D^*}^{\text{SM}}$  predictions [6, 7]

In our framework, the muonic WCs are modified in a correlated manner<sup>6</sup>,

$$\delta C_9^\mu = -\delta C_{10}^\mu = \frac{m_t^2}{16\pi\alpha_{\text{em}}} \frac{(\lambda'_{233})^2}{m_{\tilde{b}_R}^2} - \frac{\lambda'_{i23}\lambda'_{i33}\lambda'_{j23}\lambda'_{j3}}{64\sqrt{2}G_F\pi V_{tb}V_{ts}^*\alpha_{\text{em}}m_{\tilde{b}_R}^2} - \frac{\lambda'_{323}\lambda'_{333}(\lambda_{323})^2}{64\sqrt{2}G_F\pi V_{tb}V_{ts}^*\alpha_{\text{em}}} \frac{\log\left(m_{\tilde{b}_R}^2/m_{\tilde{\tau}_R}^2\right)}{m_{\tilde{b}_R}^2 - m_{\tilde{\tau}_R}^2}. \quad (16)$$

The first term corresponds to a box diagram with a  $W$  boson, a sbottom and two tops in the loop, the second to a box with two sbottoms and two tops [55] and the third to a box with a sbottom, a stau and two tau neutrinos [55]. The first two terms become negligible due to the above-mentioned constraints from the tree-level processes [58]. The third term provides the principal contribution to the anomaly and it is mainly constrained by purely leptonic processes (see next Sec. 3.2).

Box diagrams with two sbottoms and two tau neutrinos can also affect the  $B_s - \bar{B}_s$  mixing [57]. It is useful to define the effective Hamiltonian,

$$\mathcal{H}(\Delta B = 2)^{SM(NP)} = -C_{B_s}^{SM(NP)}(\bar{b}_L\gamma^\mu s_L)(\bar{b}_L\gamma_\mu s_L), \quad (17)$$

where

$$C_{B_s}^{SM} = -\frac{g^4}{128\pi^2 m_W^2}(V_{tb}V_{ts}^*)^2 S_0(m_t^2/m_W^2), \quad C_{B_s}^{NP} = \frac{\lambda'_{i23}\lambda'_{j33}\lambda'_{j23}\lambda'_{i33}}{128\pi^2 m_{\tilde{b}_R}^2}. \quad (18)$$

and  $S_0(x) = \frac{x(4-11x+x^2)}{4(1-x)^2} - \frac{3x^3 \log(x)}{2(1-x)^3}$ .

We compare the ratio,

$$C_{B_s} = \frac{|\langle B_s^0 | \mathcal{H}(\Delta B = 2)^{SM+NP} | \bar{B}_s^0 \rangle|}{|\langle B_s^0 | \mathcal{H}(\Delta B = 2)^{SM} | \bar{B}_s^0 \rangle|} = \left| 1 + \frac{C_{B_s}^{NP}}{C_{B_s}^{SM}} \right|. \quad (19)$$

with the measured value and impose similar constraints to the ones from  $R_{B \rightarrow K^{(*)}\nu\bar{\nu}}$  yet slightly weaker.

### 3.2 $Z \rightarrow \ell\bar{\ell}'$ coupling and $\tau$ decays

The main obstacles to a combined solution to the anomalies in the generic RPV scenario are the stringent constraints from the  $Z$  boson decay to a dilepton pair and the charged-current leptonic tau decay to a lepton and neutrinos [136] [137]. On the one hand, the triangle diagrams involving the sbottom and the top generate a positive contribution to the leptonic  $Z$  coupling that saturates the experimental bound already for order  $\mathcal{O}(1)$  values of  $\lambda'_{333}$ . On the other hand, the tree-level stau exchange implies an unacceptably large shift of the  $\tau \rightarrow l\nu\bar{\nu}$  decay rate [138], unless the stau mass is of order 10 TeV. The third term in 16 becomes also negligible and thus the  $R_{K^{(*)}}$  anomaly remains unresolved. Moreover, no cancellation between the positive

---

<sup>6</sup>The recent analysis in [63] considers also the likelihood in the space of pairs of WCs. It is suggested that the  $\delta C_9^\mu = -\delta C_{10}^\mu$  solution is complemented by a non-vanishing, lepton universal, negative contribution  $\delta C_9^U$ . The statistical significance of this scenario is as of now not overwhelming and we do not take it into account here. If the tendency persists, we have verified that the RPV framework can also accommodate it by the inclusion of loop-diagrams with left-handed sneutrinos. As a bonus, for light enough sneutrinos, it is possible to explain simultaneously the anomalous magnetic dipole moment of the muon [135]. The price to be paid in this case is the abandonment of our flavour symmetry, because one has to set  $\lambda'_{332}, \lambda_{332} < 10^{-4}$  in order to avoid tensions with  $B_s - \bar{B}_s$  mixing and  $\tau \rightarrow \ell\bar{\ell}'$  decays.

tree-level amplitude and the negative  $W$  penguin diagrams involving the sbottom and the top can be invoked due to the previous bounds on  $\lambda'_{333}$  from the  $Z$  coupling.

Let us write down, the observables that correspond to the two processes with contributions from both RPV and DM interactions, i.e. the ratio of  $Z$  boson axial-vector coupling,

$$\frac{a_\tau}{a_e} = 1 - \frac{3m_t^2}{16\pi^2} \frac{(\lambda'_{333})^2}{m_{\tilde{b}_R}^2} \left( \log \left( \frac{m_{\tilde{b}_R}^2}{m_t^2} \right) - 1 \right) + (1 - 4s_W^2) \frac{(\hat{\lambda}_{33})^2}{16\pi^2} \left( \frac{m_\chi^2}{m_\psi^2} \log \left( \frac{m_\chi^2}{m_\psi^2} \right) + 1 \right) \quad (20)$$

and the following ratio of leptonic decay branching ratios at leading order,

$$R_\tau^{\tau/\ell} = \frac{\mathcal{B}(\tau \rightarrow \ell\nu\bar{\nu})_{\text{exp}} / \mathcal{B}(\tau \rightarrow \ell\nu\bar{\nu})_{\text{SM}}}{\mathcal{B}(\mu \rightarrow e\nu\bar{\nu})_{\text{exp}} / \mathcal{B}(\mu \rightarrow e\nu\bar{\nu})_{\text{SM}}} \simeq 1 + \frac{\sqrt{2}}{4G_F} \frac{(\lambda_{323})^2}{m_{\tilde{\tau}_R}^2} \\ - \frac{3m_t^2}{16\pi^2} \frac{(\lambda'_{333})^2}{m_{\tilde{b}_R}^2} \left( \log \left( \frac{m_{\tilde{b}_R}^2}{m_t^2} \right) - \frac{1}{2} \right) - \frac{\hat{\lambda}_{33}\hat{\lambda}_{32}}{8\pi^2} \left( \frac{m_\chi^2}{m_\psi^2} \log \left( \frac{m_\chi^2}{m_\psi^2} \right) + 1 \right) \quad (21)$$

We observe that the inclusion of the new scalar particle  $\chi$  together with the mediator  $\psi$  can potentially improve the situation. Not only, do they enter a triangle diagram that contributes to  $\frac{a_\tau}{a_e}$  with an opposite sign to the RPV term, but also a  $W$  penguin diagram that can facilitate further the cancellation in  $R_\tau^{\tau/\ell}$ . It should be noted that, if the DM particle were the Dirac fermion in  $X_3$  the contribution to the  $Z$  coupling would be negligible. We also stress that the necessity of a cancellation between the tree-level purely leptonic interaction and the leptoquark RGE effects appearing at one-loop level is already anticipated by the general EFT analysis based on  $U(2)$  flavour symmetries [32].

In the presence of the DM interactions, the effects on two more LFV  $\tau$  decays should be taken into account. In particular,  $Z$  penguin diagrams with either the sbottom and the top [57] or the  $\chi$  and the  $\psi$  in the loop may pose a problem with regard to the SM forbidden  $\tau \rightarrow \mu\mu\bar{\mu}$  decay<sup>7</sup> and triangle diagrams with the same particles [139] [140] regarding the radiative  $\tau \rightarrow \mu\gamma$  decay. The effective Lagrangian and effective amplitude for these processes can be expressed as,

$$\mathcal{L}(\tau \rightarrow \ell\ell\bar{\ell}) = -g_{LL}^{ijk}(\bar{\tau}_L \gamma^\mu \ell_L^i)(\bar{\ell}_L^j \gamma_\mu \ell_L^k) - g_{LR}^{ijk}(\bar{\tau}_L \gamma^\mu \ell_L^i)(\bar{\ell}_R^j \gamma_\mu \ell_R^k), \quad (22)$$

$$\mathcal{M}(\tau \rightarrow \mu\gamma) = -e \frac{m_\tau}{2} \epsilon^\alpha \bar{u}_\mu [i\sigma_{\beta\alpha} q^\beta (a_R P_L + a_L P_R)] u_\tau, \quad (23)$$

We define,

$$g_{LL(LR)}^{ijk} = \frac{4\pi\alpha_{\text{em}}\kappa_{L(R)}}{c_W^2 s_W^2 m_Z^2} \left[ \frac{3m_t^2}{32\pi^2} \frac{\lambda'_{233}\lambda'_{333}}{m_{\tilde{b}_R}^2} \left( \log \left( \frac{m_{\tilde{b}_R}^2}{m_t^2} \right) - 1 \right) \right. \\ \left. - (1 - 4s_W^2) \frac{(\hat{\lambda}_{33})^2}{16\pi^2} \left( \frac{m_\chi^2}{m_\psi^2} \log \left( \frac{m_\chi^2}{m_\psi^2} \right) + 1 \right) \right]. \quad (24)$$

where  $\kappa_L = -\frac{1}{2} + s_W^2$ ,  $\kappa_R = s_W^2$  and

$$a_L = -\frac{\hat{\lambda}_{33}\hat{\lambda}_{32}}{192\pi^2 m_\psi^2} G(m_\chi^2/m_\psi^2) - \frac{\lambda'_{2i3}\lambda'_{3i3}}{64\pi^2 m_{\tilde{b}_R}^2}, \quad a_R = 0, \quad (25)$$

---

<sup>7</sup>There are also box diagrams [57] and photon penguin [139] diagrams that contribute to this decay but we have explicitly checked that they are subleading.

where  $G(x) = \frac{1}{(1-x)^4}(2 - 3x - 6x^2 + x^3 + 6x \log(x))$ . The branching ratios [141],

$$\begin{aligned} \mathcal{B}(\tau \rightarrow \mu\mu\bar{\mu}) &= \frac{1}{G_F^2} \left[ \frac{(g_{LL}^{3\mu})^2 + (g_{LR}^{3\mu})^2}{4} + \left( \log \frac{m_\tau^2}{m_\mu^2} - \frac{11}{4} \right) (4\pi\alpha_{\text{em}})^2 a_L^2 \right. \\ &\quad \left. + \left( g_{LL}^{3\mu} + \frac{1}{2} g_{LR}^{3\mu} \right) (4\pi\alpha_{\text{em}}) a_L \right] \mathcal{B}(\tau \rightarrow \mu\bar{\nu}_\mu\nu_\tau) \end{aligned} \quad (26)$$

$$\mathcal{B}(\tau \rightarrow \mu\gamma) = \frac{48\pi^3\alpha_{\text{em}}}{G_F^2} (a_L^2 + a_R^2) \mathcal{B}(\tau \rightarrow \mu\bar{\nu}_\mu\nu_\tau) \quad (27)$$

must then comply with the respective experimental upper bounds.

### 3.3 Relic abundance and Dark Matter direct detection

The DM particle couples directly to leptons and therefore the main self-annihilation channels are  $\bar{\chi}\chi \rightarrow \ell\ell$  and  $\bar{\chi}\chi \rightarrow \bar{\nu}_\ell\nu_\ell$  with  $\ell = \mu, \tau$ . Because  $\chi$  is a scalar particle, the effective cross-section is p-wave suppressed [83],

$$\frac{1}{2} \langle \sigma v \rangle = \frac{1}{2} \left[ \frac{(\hat{\lambda}_{32}^2 + \hat{\lambda}_{33}^2)m_\chi^2}{48\pi(m_\psi^2 + m_\chi^2)^2} v^2 \right] \equiv p v^2 \quad (28)$$

where  $v \sim 3$  is the DM velocity at freeze-out. The relic abundance can be estimated following the calculation in Ref. [70]. Co-annihilation effects are irrelevant since the rest of the DM generations are taken to be heavier.

Concerning direct detection, the dominant contribution for DM scattering off nucleons is generated via a penguin diagram involving leptons and the charged mediator in the loop and a virtual photon exchange. The respective dimension-6 operator is called charge-radius operator,

$$\mathcal{L}_{\text{charge-radius}} = i b_\chi \partial_\mu \chi^* \partial_\nu \chi F^{\mu\nu}, \quad (29)$$

where

$$b_\chi = \sum_{\ell=\mu,\tau} \frac{\hat{\lambda}_{3\ell}^2 e}{16\pi^2 m_\psi^2} \left( 1 - \frac{2}{3} \log \left( \frac{m_\ell^2}{m_\psi^2} \right) \right). \quad (30)$$

The spin-independent DM-nucleus differential scattering cross section is then [83],

$$\frac{d\sigma}{dE_R} = \frac{Z^2 e^2 b_\chi^2 m_T}{16\pi v^2} F_E^2(q^2). \quad (31)$$

Here,  $E_R = |\vec{q}|^2 / 2m_T$  is the recoil energy;  $v$  is the DM velocity in the lab frame;  $m_T$  is the mass,  $Z$  the atomic number and  $F_E(q^2)$  the electric form factor of the target nucleus [142]. Eq. 31 has the same  $E_R$ - and  $v^2$ -dependence as the ordinary spin-independent cross section for a contact interaction, we can directly map the latest, most stringent exclusion limits, as published by the XENON1T collaboration [143], onto limits on the parameter space of the current model. Since, the virtual photon couples only to protons inside the nucleus, a rescaling with  $Z^2/A^2$  is necessary in order to account for the resulting isospin violation. We also derive projections for XENONnT, which is the next upgrade step of XENON1T and will increase the target mass to  $5.9t$ , by assuming the same efficiency profile.

Lastly, we mention that indirect detection signals of scalar DM are too small to be observed due to the p-wave suppression of the cross-section [144].

### 3.4 Collider searches

We highlight the basic aspects of the high- $p_T$  searches for the new particles. The direct comparison with analyses that study the analogous EFT operators offers the possibility to set present and future bounds for their masses and interactions.

- **$\tilde{b}_R$ .** Crossing symmetry dictates that an explanation for  $R_{D^{(*)}}$  is unambiguously connected to the scattering  $bc \rightarrow \tau\bar{\nu}$ . The data from the mono-tau signature  $pp \rightarrow \tau_h X + \text{MET}$  at LHC set upper bounds on the WC of the effective operator generated by a scalar leptoquark  $S_1 \sim (\bar{\mathbf{3}}, \mathbf{1})_{1/3}$  exchange [56] [145], which for our case translate into  $\Delta_{33}^c < 0.32$  (see Eq. 12). The prognosis for the HL-LHC ( $3000 \text{ fb}^{-1}$ ) gives  $\Delta_{33}^c < 0.1$ .
- **$\tilde{\tau}_R$ .** Depending on the nature of the LSP, the possible signatures involving the stau are classified in Ref. [146]. The best limits in RPV searches using simplified models yield  $m_{\tilde{\tau}_R} > 300 \text{ GeV}$ .
- **$\chi$  &  $\psi$ .** The mediator  $\psi$  can be pair-produced at LHC via Drell-Yan processes, i.e. a  $Z$  boson or photon exchange, with di-lepton plus missing energy signature  $l_i^+ l_j^- + \text{MET}$ . The cross sections is larger than that of fermion DM models, because there are more helicity states for the fermionic mediator. If the leptons have the same flavour, one can recast slepton searches and extrapolate the limits:  $m_\chi > 300 \text{ GeV}$  and  $m_\psi > 500 \text{ GeV}$  [84]. Likewise,  $\psi\bar{\psi}$  direct production is possible at LEP, but the bounds are even weaker [144]. Other channels accessible at future muon colliders that are relevant to our setup could be  $\mu^+\mu^- \rightarrow \chi\bar{\chi}\gamma$  at tree-level with mono-photon search signature and  $\mu^+\mu^- \rightarrow l_i^+ l_j^- \gamma$  at one-loop level with multi-flavour lepton final state (in analogy to the discussion in Ref. [89] for LEP).

## 4 Phenomenological Analysis

The preferred region of the parameter space is determined by performing a minimization of the  $\chi^2$ -distribution composed by the observables of the previous Section 3. We use the experimental data of Table 2, the XENON1T exclusion limits [143], the mass lower bounds set by collider searches (see Sec. 3.4) and the necessary SM input [132]. The best-fit point is presented in Table 3. It can be inferred that the predicted parameter sizes are natural and, despite some couplings are large, they are within the unitarity bound of  $\sqrt{4\pi}$ . The improvement of the total  $\chi^2$  with respect to the SM limit is remarkable  $\chi^2(x_{\text{SM}}) - \chi^2(x_{\text{BF}}) \simeq 47 - 5 = 42$ , practically reflecting the complete resolution of the anomalies. This is also evident in the Figures 1, where the 68% CL and 95% CL regions of the  $r_{D^{(*)}}$  and  $\delta C_9^\mu$  observables in the  $(\lambda'_{333}, \lambda'_{323})$ ,  $(\lambda'_{333}, m_{\tilde{b}_R})$ ,  $(\lambda'_{323}, m_{\tilde{b}_R})$  and  $(\lambda'_{333}, m_{\tilde{\tau}_R})$  planes are shown together with the  $2\sigma$  exclusion contours from the other low-energy observables.

RPV & DM couplings	best-fit point	Flavour Suppression	Total value
$\lambda_{323}$	3.5	$\epsilon_{\bar{F}}$	3.5
$\lambda'_{223}$	$1^\dagger$	$\epsilon_{\bar{F}}\epsilon$	0.03
$\lambda'_{233}$	0.7	$\epsilon_{\bar{F}}$	0.7
$\lambda'_{323}$	2.4	$\epsilon$	0.07
$\lambda'_{333}$	2.3	1	2.3
$\hat{\lambda}_{32}$	$1^\dagger$	$\epsilon_{\bar{F}}$	1
$\hat{\lambda}_{33}$	3.5	1	3.5

Masses	best-fit point [TeV]
$m_{\tilde{b}_R}$	1450
$m_{\tilde{\tau}_R}$	2900
$m_\chi$	700
$m_\psi$	1950

Table 3: The best-fit point for the couplings along with the flavour suppression factors and the particle masses. The entries marked with a dagger are not determined by the fit, but are rather benchmark points (see text).

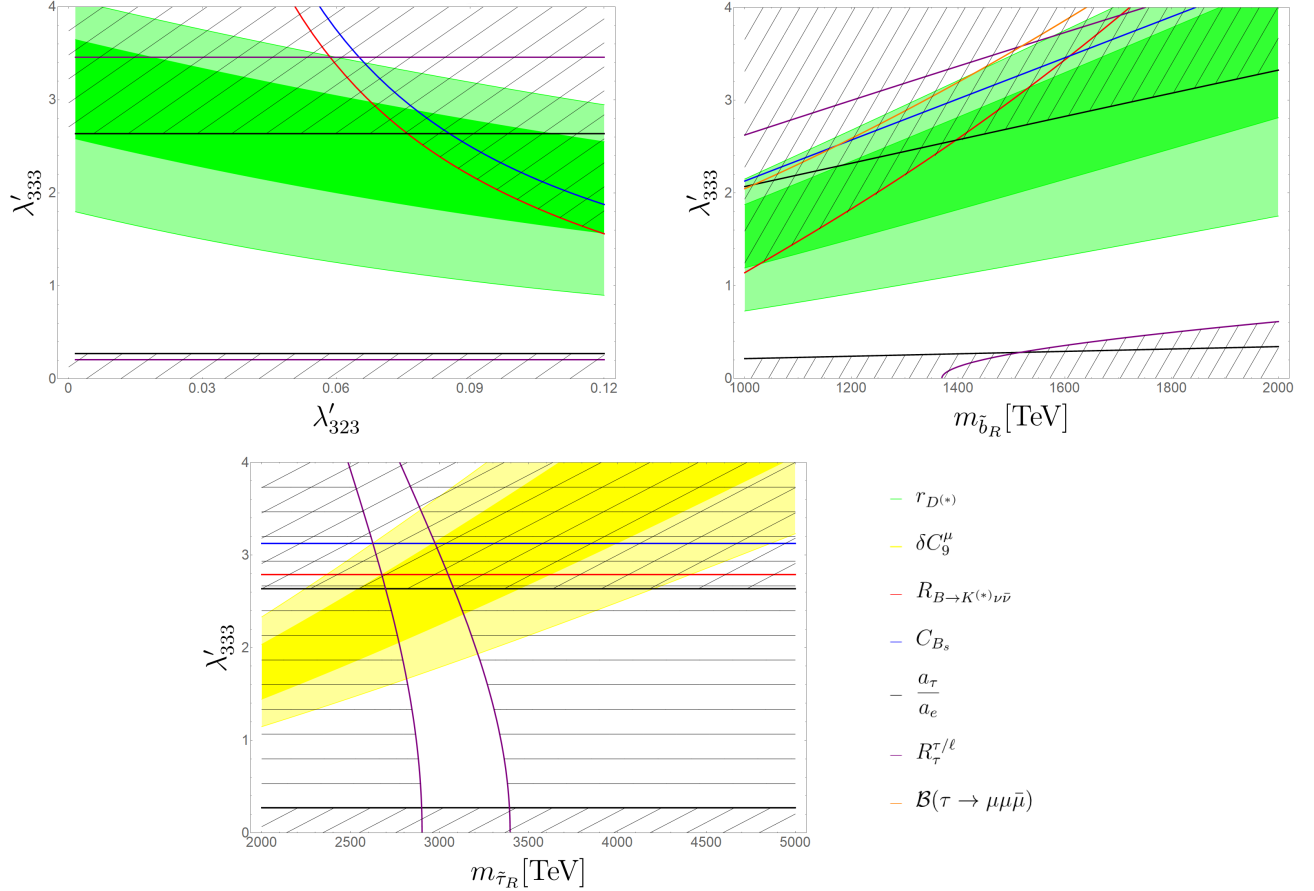


Figure 1: RPV parameter space compatible with a solution for  $r_{D^{(*)}}$  (green) and  $\delta C_9^\mu$  (yellow) at  $1\sigma$  and  $2\sigma$  around the best-fit point. The hatched region is excluded at  $2\sigma$  due to the following constraints:  $R_{B \rightarrow K^{(*)}\nu\bar{\nu}}$  (red),  $C_{B_s}$  (blue),  $\frac{a_\tau}{a_e}$  (black),  $R_\tau^{\tau/\ell}$  (purple),  $\mathcal{B}(\tau \rightarrow \mu\mu\bar{\mu})$  (orange).

We observe that a large fraction of the parameter space becomes available due the cancellation mechanism in  $\frac{a_\tau}{a_e}$  and  $R_\tau^{\tau/\ell}$ , which occurs roughly at the 40%- and 10%-level independently of the relative sign of the couplings. In particular, the coupling  $\lambda'_{333}$  reaches now higher values compared with the generic RPV scenario [56] and the bounds on  $B_s - \bar{B}_s$  mixing and  $R_{B \rightarrow K^{(*)}\nu\bar{\nu}}$  are still satisfied thanks to the flavour suppression in  $\lambda'_{323}$ . Moreover, the stau can be relatively light enhancing adequately the last term in Eq. 16. Both  $R_{D^{(*)}}$  and  $R_{K^{(*)}}$  are then in good agreement with the present central values and the mass spectrum is more natural with all the right-handed superpartners,  $\chi$  and  $\psi$  within the same mass range of a few TeV. However, due to the sensitivity of  $R_\tau^{\tau/\ell}$  to the cancellation,  $R_{K^{(*)}}$  can only be accommodated in a concrete band of the  $(\lambda'_{333}, m_{\tilde{\tau}_R})$  plane, which for this solution is located around a stau mass of approximately 3 TeV. By varying the coupling  $2.5 \lesssim \lambda_{323} \leq 3.5$ , the position of the band can be moved to the left as low as 2 TeV before abandoning the  $1\sigma$  region for  $\delta C_9^\mu$ . As for the couplings  $\lambda'_{223}$  and  $\lambda'_{233}$ , the first is flavour suppressed and does not affect the fit and the latter is primarily constrained by the bounds on LFV  $\tau$  decays (see Eqs. 22-27).

Regarding the DM interactions, we notice that the coupling  $\hat{\lambda}_{32}$  appears only in a product combination with the coupling  $\hat{\lambda}_{33}$  in the observables of Sec. 3.2 and the single-coupling bounds from e.g.  $\frac{a_\mu}{a_e}$ , are satisfied for any order  $\mathcal{O}(1)$  value. Consequently, it is convenient to use the benchmark  $\hat{\lambda}_{32} = 1$  and include only  $\hat{\lambda}_{33}$  in the fit. The region in the  $(m_\psi, m_\chi)$  plane that can give rise to the correct relic abundance is shown in Figure 2. The present direct detection and LFV bounds allow for a DM mass  $700 \text{ GeV} < m_\chi < 1.5 \text{ TeV}$  and we have explicitly verified that the cancellation mechanism is applicable for the whole mass range by readjusting the rest of the parameters in the vicinity of the best-fit point.

As a final note, we comment on the testability of the model by future experiments. With the most recent world average for the charged-current anomalies [5], we calculate  $\Delta_{33}^c \approx 0.065$ . The ‘no-loose theorem’ of Ref. [145] no longer applies and there is still an open window for the leptoquark explanation of  $R_{D^{(*)}}$ , even if there is no discovery after the HL-LHC phase. The situation for the stau and  $\chi$  is even more inconclusive, since the best-fit point masses for these particles appear to be out of reach of the LHC. On the other hand, DM direct detection looks much more promising. We see that the bulk of the parameter space for the chosen benchmark will be probed by XENONnT (and other experiments that aim at similar exposure). If the anomalies are univocally confirmed as NP signals, it is worth analysing the sensitivity of the next generation of colliders to the heavy particles predicted by the model.

## 5 Conclusions

In this paper, we aspire to restore the connection between SUSY and WIMP DM physics, even in the case that R-parity is violated. As pathfinder we use the hypothesis that the hidden sector is flavoured and combined with the RPV interactions may underlie the NP effects related to the B-physics anomalies. In fact, the model provides an explanation for the  $R_{D^{(*)}}$  and  $R_{K^{(*)}}$  anomalies without raising significant tensions with other low-energy observables partially due to a destructive amplitude interference between the RPV and DM interactions. The above, as well as the compliance with all the requirements of DM phenomenology successfully occur for a natural choice of parameters and mass spectrum. We also commit ourselves to a well-motivated  $U(2)^2$  flavour symmetry that consistently describes the SM Yukawa, RPV and DM coupling hierarchies. It is ensured that all newly introduced particles, interactions and symmetry breaking

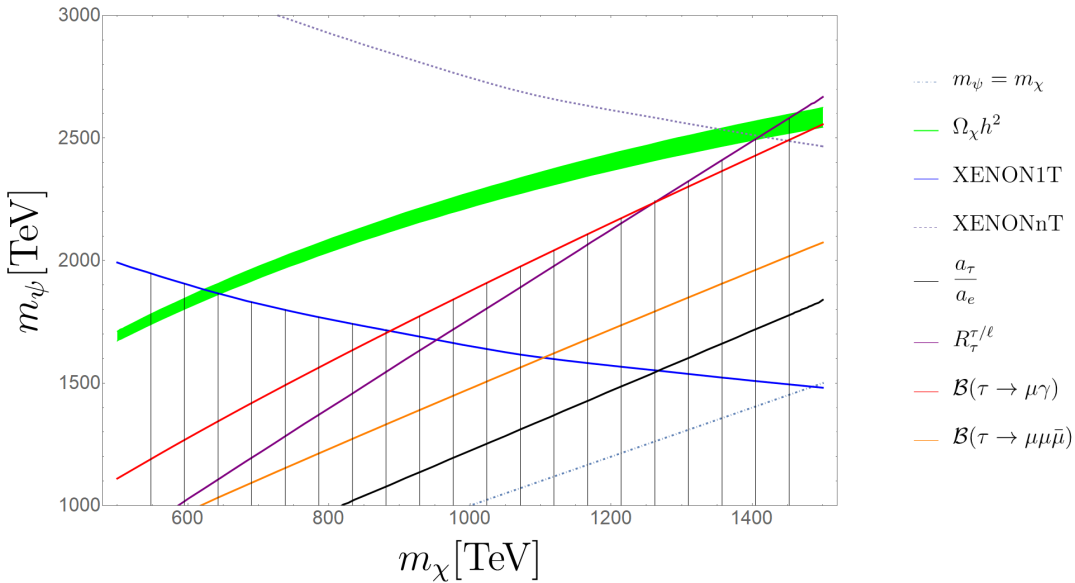


Figure 2: DM parameter space compatible with the correct relic abundance (green) at  $1\sigma$  around the best-fit point. The hatched region is excluded at  $2\sigma$  due to the following constraints: XENON1T exclusion limits (blue),  $\frac{a_\tau}{a_e}$  (black),  $R_\tau^{\tau/\ell}$  (purple),  $\mathcal{B}(\tau \rightarrow \mu\gamma)$  (red),  $\mathcal{B}(\tau \rightarrow \mu\mu\bar{\mu})$  (orange). The dashed line represents the prospective XENONnT exclusion limits.

patterns are in accordance with the spirit of gauge coupling unification. If the sbottom is the LSP, SUSY may remain elusive for the LHC, whereas experimental validation of the proposed DM interaction by direct detection searches can be expected in the near future.

## Acknowledgements

We thank Gino Isidori, Javier Fuentes-Martin and Michael Baker for useful discussions and comments on the manuscript. This research was supported in part by the Swiss National Science Foundation (SNF) under contract 200021-159720.

## References

- [1] BaBar, J. P. Lees *et al.*, *Phys. Rev.* **D88** (2013) no. 7, 072012, [arXiv:1303.0571 \[hep-ex\]](https://arxiv.org/abs/1303.0571).
- [2] Belle, S. Hirose *et al.*, [arXiv:1612.00529 \[hep-ex\]](https://arxiv.org/abs/1612.00529).
- [3] LHCb, R. Aaij *et al.*, *Phys. Rev. Lett.* **115** (2015) no. 11, 111803, [arXiv:1506.08614 \[hep-ex\]](https://arxiv.org/abs/1506.08614). [Addendum: *Phys. Rev. Lett.* 115,no.15,159901(2015)].
- [4] LHCb, R. Aaij *et al.*, *Phys. Rev.* **D97** (2018) no. 7, 072013, [arXiv:1711.02505 \[hep-ex\]](https://arxiv.org/abs/1711.02505).
- [5] Belle, G. Caria. [http://moriond.in2p3.fr/2019/EW/slides/6\\_Friday/3\\_YSF/1\\_gcaria\\_moriond2019.pdf](http://moriond.in2p3.fr/2019/EW/slides/6_Friday/3_YSF/1_gcaria_moriond2019.pdf).
- [6] F. U. Bernlochner, Z. Ligeti, M. Papucci, and D. J. Robinson, *Phys. Rev.* **D95** (2017) no. 11, 115008, [arXiv:1703.05330 \[hep-ph\]](https://arxiv.org/abs/1703.05330). [Erratum: *Phys. Rev.* D97,no.5,059902(2018)].

- [7] D. Bigi, P. Gambino, and S. Schacht, *JHEP* **11** (2017) 061, [arXiv:1707.09509 \[hep-ph\]](#).
- [8] **LHCb**, R. Aaij *et al.*, *JHEP* **08** (2017) 055, [arXiv:1705.05802 \[hep-ex\]](#).
- [9] **LHCb**, R. Aaij *et al.*, [arXiv:1903.09252 \[hep-ex\]](#).
- [10] M. Bordone, G. Isidori, and A. Patti, *Eur. Phys. J.* **C76** (2016) no. 8, 440, [arXiv:1605.07633 \[hep-ph\]](#).
- [11] **LHCb**, R. Aaij *et al.*, *JHEP* **02** (2016) 104, [arXiv:1512.04442 \[hep-ex\]](#).
- [12] **Belle**, S. Wehle *et al.*, [arXiv:1612.05014 \[hep-ex\]](#).
- [13] M. Ciuchini, M. Fedele, E. Franco, S. Mishima, A. Paul, L. Silvestrini, and M. Valli, *JHEP* **06** (2016) 116, [arXiv:1512.07157 \[hep-ph\]](#).
- [14] **LHCb**, R. Aaij *et al.*, *Phys. Rev. Lett.* **120** (2018) no. 12, 121801, [arXiv:1711.05623 \[hep-ex\]](#).
- [15] R. Watanabe *Phys. Lett.* **B776** (2018) 5–9, [arXiv:1709.08644 \[hep-ph\]](#).
- [16] B. Bhattacharya, A. Datta, D. London, and S. Shivashankara, *Phys. Lett.* **B742** (2015) 370–374, [arXiv:1412.7164 \[hep-ph\]](#).
- [17] R. Alonso, B. Grinstein, and J. Martin Camalich, *JHEP* **10** (2015) 184, [arXiv:1505.05164 \[hep-ph\]](#).
- [18] A. Greljo, G. Isidori, and D. Marzocca, *JHEP* **07** (2015) 142, [arXiv:1506.01705 \[hep-ph\]](#).
- [19] L. Calibbi, A. Crivellin, and T. Ota, *Phys. Rev. Lett.* **115** (2015) 181801, [arXiv:1506.02661 \[hep-ph\]](#).
- [20] M. Bauer and M. Neubert, *Phys. Rev. Lett.* **116** (2016) no. 14, 141802, [arXiv:1511.01900 \[hep-ph\]](#).
- [21] S. Fajfer and N. Ko?nik, *Phys. Lett.* **B755** (2016) 270–274, [arXiv:1511.06024 \[hep-ph\]](#).
- [22] R. Barbieri, G. Isidori, A. Patti, and F. Senia, *Eur. Phys. J.* **C76** (2016) no. 2, 67, [arXiv:1512.01560 \[hep-ph\]](#).
- [23] D. Das, C. Hati, G. Kumar, and N. Mahajan, *Phys. Rev.* **D94** (2016) 055034, [arXiv:1605.06313 \[hep-ph\]](#).
- [24] G. Hiller, D. Loose, and K. Schoenwald, *JHEP* **12** (2016) 027, [arXiv:1609.08895 \[hep-ph\]](#).
- [25] B. Bhattacharya, A. Datta, J.-P. Guévin, D. London, and R. Watanabe, *JHEP* **01** (2017) 015, [arXiv:1609.09078 \[hep-ph\]](#).
- [26] S. M. Boucenna, A. Celis, J. Fuentes-Martin, A. Vicente, and J. Virto, *Phys. Lett.* **B760** (2016) 214–219, [arXiv:1604.03088 \[hep-ph\]](#).
- [27] D. Buttazzo, A. Greljo, G. Isidori, and D. Marzocca, *JHEP* **08** (2016) 035, [arXiv:1604.03940 \[hep-ph\]](#).
- [28] S. M. Boucenna, A. Celis, J. Fuentes-Martin, A. Vicente, and J. Virto, *JHEP* **12** (2016) 059, [arXiv:1608.01349 \[hep-ph\]](#).
- [29] R. Barbieri, C. W. Murphy, and F. Senia, *Eur. Phys. J.* **C77** (2017) no. 1, 8, [arXiv:1611.04930 \[hep-ph\]](#).
- [30] D. Becirevic, N. Kosnik, O. Sumensari, and R. Zukanovich Funchal, *JHEP* **11** (2016) 035, [arXiv:1608.07583 \[hep-ph\]](#).
- [31] D. Buttazzo, A. Greljo, G. Isidori, and D. Marzocca, *JHEP* **11** (2017) 044, [arXiv:1706.07808 \[hep-ph\]](#).
- [32] M. Bordone, G. Isidori, and S. Trifinopoulos, *Phys. Rev.* **D96** (2017) no. 1, 015038, [arXiv:1702.07238 \[hep-ph\]](#).

- [33] A. Crivellin, D. Müller, and T. Ota, *JHEP* **09** (2017) 040, [arXiv:1703.09226 \[hep-ph\]](#).
- [34] Y. Cai, J. Gargalionis, M. A. Schmidt, and R. R. Volkas, *JHEP* **10** (2017) 047, [arXiv:1704.05849 \[hep-ph\]](#).
- [35] E. Megias, M. Quiros, and L. Salas, *JHEP* **07** (2017) 102, [arXiv:1703.06019 \[hep-ph\]](#).
- [36] L. Di Luzio, A. Greljo, and M. Nardecchia, *Phys. Rev.* **D96** (2017) no. 11, 115011, [arXiv:1708.08450 \[hep-ph\]](#).
- [37] N. Assad, B. Fornal, and B. Grinstein, *Phys. Lett.* **B777** (2018) 324–331, [arXiv:1708.06350 \[hep-ph\]](#).
- [38] L. Calibbi, A. Crivellin, and T. Li, [arXiv:1709.00692 \[hep-ph\]](#).
- [39] M. Bordone, C. Cornella, J. Fuentes-Martin, and G. Isidori, *Phys. Lett.* **B779** (2018) 317–323, [arXiv:1712.01368 \[hep-ph\]](#).
- [40] R. Barbieri and A. Tesi, *Eur. Phys. J.* **C78** (2018) no. 3, 193, [arXiv:1712.06844 \[hep-ph\]](#).
- [41] A. Greljo and B. A. Stefanek, *Phys. Lett.* **B782** (2018) 131–138, [arXiv:1802.04274 \[hep-ph\]](#).
- [42] M. Blanke and A. Crivellin, *Phys. Rev. Lett.* **121** (2018) no. 1, 011801, [arXiv:1801.07256 \[hep-ph\]](#).
- [43] L. Di Luzio, J. Fuentes-Martin, A. Greljo, M. Nardecchia, and S. Renner, *JHEP* **11** (2018) 081, [arXiv:1808.00942 \[hep-ph\]](#).
- [44] D. Marzocca *JHEP* **07** (2018) 121, [arXiv:1803.10972 \[hep-ph\]](#).
- [45] J. Kumar, D. London, and R. Watanabe, *Phys. Rev.* **D99** (2019) no. 1, 015007, [arXiv:1806.07403 \[hep-ph\]](#).
- [46] D. Guadagnoli, M. Reboud, and O. Sumensari, *JHEP* **11** (2018) 163, [arXiv:1807.03285 \[hep-ph\]](#).
- [47] D. Becirevic, I. Dorsner, S. Fajfer, N. Kosnik, D. A. Faroughy, and O. Sumensari, [arXiv:1806.05689 \[hep-ph\]](#).
- [48] M. Bordone, C. Cornella, J. Fuentes-Martin, and G. Isidori, *JHEP* **10** (2018) 148, [arXiv:1805.09328 \[hep-ph\]](#).
- [49] B. Fornal, S. A. Gadom, and B. Grinstein, *Phys. Rev.* **D99** (2019) no. 5, 055025, [arXiv:1812.01603 \[hep-ph\]](#).
- [50] S. Bhattacharya, A. Biswas, Z. Calcuttawala, and S. K. Patra, [arXiv:1902.02796 \[hep-ph\]](#).
- [51] C. Cornella, J. Fuentes-Martin, and G. Isidori, [arXiv:1903.11517 \[hep-ph\]](#).
- [52] S. Biswas, D. Chowdhury, S. Han, and S. J. Lee, *JHEP* **02** (2015) 142, [arXiv:1409.0882 \[hep-ph\]](#).
- [53] J. Zhu, H.-M. Gan, R.-M. Wang, Y.-Y. Fan, Q. Chang, and Y.-G. Xu, *Phys. Rev.* **D93** (2016) no. 9, 094023, [arXiv:1602.06491 \[hep-ph\]](#).
- [54] N. G. Deshpande and X.-G. He, *Eur. Phys. J.* **C77** (2017) no. 2, 134, [arXiv:1608.04817 \[hep-ph\]](#).
- [55] D. Das, C. Hati, G. Kumar, and N. Mahajan, *Phys. Rev.* **D96** (2017) no. 9, 095033, [arXiv:1705.09188 \[hep-ph\]](#).
- [56] W. Altmannshofer, P. Bhupal Dev, and A. Soni, *Phys. Rev.* **D96** (2017) no. 9, 095010, [arXiv:1704.06659 \[hep-ph\]](#).
- [57] K. Earl and T. Gregoire, [arXiv:1806.01343 \[hep-ph\]](#).

- [58] S. Trifinopoulos *Eur. Phys. J.* **C78** (2018) no. 10, 803, arXiv:1807.01638 [hep-ph].
- [59] Q.-Y. Hu, X.-Q. Li, Y. Muramatsu, and Y.-D. Yang, *Phys. Rev.* **D99** (2019) no. 1, 015008, arXiv:1808.01419 [hep-ph].
- [60] R. Barbieri and R. Ziegler, arXiv:1904.04121 [hep-ph].
- [61] S. Descotes-Genon, L. Hofer, J. Matias, and J. Virto, *JHEP* **06** (2016) 092, arXiv:1510.04239 [hep-ph].
- [62] W. Altmannshofer, P. Stangl, and D. M. Straub, *Phys. Rev.* **D96** (2017) no. 5, 055008, arXiv:1704.05435 [hep-ph].
- [63] J. Aebischer, W. Altmannshofer, D. Guadagnoli, M. Reboud, P. Stangl, and D. M. Straub, arXiv:1903.10434 [hep-ph].
- [64] S. P. Martin arXiv:hep-ph/9709356 [hep-ph]. [Adv. Ser. Direct. High Energy Phys.18,1(1998)].
- [65] R. Barbieri, G. R. Dvali, and L. J. Hall, *Phys. Lett.* **B377** (1996) 76–82, arXiv:hep-ph/9512388 [hep-ph].
- [66] R. Barbieri, G. Isidori, J. Jones-Perez, P. Lodone, and D. M. Straub, *Eur. Phys. J.* **C71** (2011) 1725, arXiv:1105.2296 [hep-ph].
- [67] J. F. Kamenik and J. Zupan, *Phys. Rev.* **D84** (2011) 111502, arXiv:1107.0623 [hep-ph].
- [68] J. Kile and A. Soni, *Phys. Rev.* **D84** (2011) 035016, arXiv:1104.5239 [hep-ph].
- [69] B. Batell, J. Pradler, and M. Spannowsky, *JHEP* **08** (2011) 038, arXiv:1105.1781 [hep-ph].
- [70] Y. Bai and J. Berger, *JHEP* **11** (2013) 171, arXiv:1308.0612 [hep-ph].
- [71] B. Batell, T. Lin, and L.-T. Wang, *JHEP* **01** (2014) 075, arXiv:1309.4462 [hep-ph].
- [72] A. Kumar and S. Tulin, *Phys. Rev.* **D87** (2013) no. 9, 095006, arXiv:1303.0332 [hep-ph].
- [73] A. DiFranzo, K. I. Nagao, A. Rajaraman, and T. M. P. Tait, *JHEP* **11** (2013) 014, arXiv:1308.2679 [hep-ph]. [Erratum: JHEP01,162(2014)].
- [74] L. Lopez-Honorez and L. Merlo, *Phys. Lett.* **B722** (2013) 135–143, arXiv:1303.1087 [hep-ph].
- [75] P. Agrawal, B. Batell, D. Hooper, and T. Lin, *Phys. Rev.* **D90** (2014) no. 6, 063512, arXiv:1404.1373 [hep-ph].
- [76] P. Agrawal, M. Blanke, and K. Gemmeler, *JHEP* **10** (2014) 072, arXiv:1405.6709 [hep-ph].
- [77] C. Kilic, M. D. Klimek, and J.-H. Yu, *Phys. Rev.* **D91** (2015) no. 5, 054036, arXiv:1501.02202 [hep-ph].
- [78] M. Blanke and S. Kast, *JHEP* **05** (2017) 162, arXiv:1702.08457 [hep-ph].
- [79] M. Blanke, S. Das, and S. Kast, *JHEP* **02** (2018) 105, arXiv:1711.10493 [hep-ph].
- [80] P. Agrawal, S. Blanchet, Z. Chacko, and C. Kilic, *Phys. Rev.* **D86** (2012) 055002, arXiv:1109.3516 [hep-ph].
- [81] P. Agrawal, Z. Chacko, and C. B. Verhaaren, *JHEP* **08** (2014) 147, arXiv:1402.7369 [hep-ph].
- [82] Z.-H. Yu, X.-J. Bi, Q.-S. Yan, and P.-F. Yin, *Phys. Rev.* **D91** (2015) no. 3, 035008, arXiv:1410.3347 [hep-ph].
- [83] Y. Bai and J. Berger, *JHEP* **08** (2014) 153, arXiv:1402.6696 [hep-ph].

- [84] S. Chang, R. Edezhath, J. Hutchinson, and M. Luty, *Phys. Rev.* **D90** (2014) no. 1, 015011, [arXiv:1402.7358 \[hep-ph\]](#).
- [85] J. Kile, A. Kobach, and A. Soni, *Phys. Lett.* **B744** (2015) 330–338, [arXiv:1411.1407 \[hep-ph\]](#).
- [86] A. Hamze, C. Kilic, J. Koeller, C. Trendafilova, and J.-H. Yu, *Phys. Rev.* **D91** (2015) no. 3, 035009, [arXiv:1410.3030 \[hep-ph\]](#).
- [87] C.-J. Lee and J. Tandean, *JHEP* **04** (2015) 174, [arXiv:1410.6803 \[hep-ph\]](#).
- [88] P. Agrawal, Z. Chacko, E. C. F. S. Fortes, and C. Kilic, *Phys. Rev.* **D93** (2016) no. 10, 103510, [arXiv:1511.06293 \[hep-ph\]](#).
- [89] M.-C. Chen, J. Huang, and V. Takhistov, *JHEP* **02** (2016) 060, [arXiv:1510.04694 \[hep-ph\]](#).
- [90] M. J. Baker and A. Thamm, *JHEP* **10** (2018) 187, [arXiv:1806.07896 \[hep-ph\]](#).
- [91] D. Aristizabal Sierra, F. Staub, and A. Vicente, *Phys. Rev.* **D92** (2015) no. 1, 015001, [arXiv:1503.06077 \[hep-ph\]](#).
- [92] G. Belanger, C. Delaunay, and S. Westhoff, *Phys. Rev.* **D92** (2015) 055021, [arXiv:1507.06660 \[hep-ph\]](#).
- [93] J. Kawamura, S. Okawa, and Y. Omura, *Phys. Rev.* **D96** (2017) no. 7, 075041, [arXiv:1706.04344 \[hep-ph\]](#).
- [94] P. Ko, T. Nomura, and H. Okada, *Phys. Lett.* **B772** (2017) 547–552, [arXiv:1701.05788 \[hep-ph\]](#).
- [95] K. Fuyuto, H.-L. Li, and J.-H. Yu, *Phys. Rev.* **D97** (2018) no. 11, 115003, [arXiv:1712.06736 \[hep-ph\]](#).
- [96] J. M. Cline *Phys. Rev.* **D97** (2018) no. 1, 015013, [arXiv:1710.02140 \[hep-ph\]](#).
- [97] J. M. Cline and J. M. Cornell, *Phys. Lett.* **B782** (2018) 232–237, [arXiv:1711.10770 \[hep-ph\]](#).
- [98] A. Azatov, D. Barducci, D. Ghosh, D. Marzocca, and L. Ubaldi, *JHEP* **10** (2018) 092, [arXiv:1807.10745 \[hep-ph\]](#).
- [99] P. Rocha-Moran and A. Vicente, *Phys. Rev.* **D99** (2019) no. 3, 035016, [arXiv:1810.02135 \[hep-ph\]](#).
- [100] N. Bernal, D. Restrepo, C. Yaguna, and s. Zapata, *Phys. Rev.* **D99** (2019) no. 1, 015038, [arXiv:1808.03352 \[hep-ph\]](#).
- [101] L. Darme, K. Kowalska, L. Roszkowski, and E. M. Sessolo, *JHEP* **10** (2018) 052, [arXiv:1806.06036 \[hep-ph\]](#).
- [102] S.-M. Choi, Y.-J. Kang, H. M. Lee, and T.-G. Ro, *JHEP* **10** (2018) 104, [arXiv:1807.06547 \[hep-ph\]](#).
- [103] G. Kumar, C. Hati, J. Orloff, and A. M. Teixeira, in *16th Conference on Flavor Physics and CP Violation (FPCP 2018) Hyderabad, INDIA, July 14-18, 2018*. 2018. [arXiv:1811.10927 \[hep-ph\]](#).
- [104] S. Singirala, S. Sahoo, and R. Mohanta, *Phys. Rev.* **D99** (2019) no. 3, 035042, [arXiv:1809.03213 \[hep-ph\]](#).
- [105] C. Hati, G. Kumar, J. Orloff, and A. M. Teixeira, *JHEP* **11** (2018) 011, [arXiv:1806.10146 \[hep-ph\]](#).
- [106] A. Falkowski, S. F. King, E. Perdomo, and M. Pierre, *JHEP* **08** (2018) 061, [arXiv:1803.04430 \[hep-ph\]](#).
- [107] N. Okada, S. Okada, and D. Raut, [arXiv:1811.11927 \[hep-ph\]](#).
- [108] S. Baek and C. Yu, *JHEP* **11** (2018) 054, [arXiv:1806.05967 \[hep-ph\]](#).

- [109] P. T. P. Hutaurok, T. Nomura, H. Okada, and Y. Orikasa, *Phys. Rev.* **D99** (2019) no. 5, 055041, [arXiv:1901.03932 \[hep-ph\]](#).
- [110] A. Biswas and A. Shaw, [arXiv:1903.08745 \[hep-ph\]](#).
- [111] D. G. Cerdeno, A. Cheek, P. Martin-Ramiro, and J. M. Moreno, [arXiv:1902.01789 \[hep-ph\]](#).
- [112] S. Baek [arXiv:1901.04761 \[hep-ph\]](#).
- [113] R. Barbier *et al.*, *Phys. Rept.* **420** (2005) 1–202, [arXiv:hep-ph/0406039 \[hep-ph\]](#).
- [114] C. Brust, A. Katz, S. Lawrence, and R. Sundrum, *JHEP* **03** (2012) 103, [arXiv:1110.6670 \[hep-ph\]](#).
- [115] C. Smith in *Proceedings, 34th International Conference on High Energy Physics (ICHEP 2008): Philadelphia, Pennsylvania, July 30-August 5, 2008*. 2008. [arXiv:0809.3152 \[hep-ph\]](#).
- [116] C. Csaki, Y. Grossman, and B. Heidenreich, *Phys. Rev.* **D85** (2012) 095009, [arXiv:1111.1239 \[hep-ph\]](#).
- [117] C. Autermann *Prog. Part. Nucl. Phys.* **90** (2016) 125–155, [arXiv:1609.01686 \[hep-ex\]](#).
- [118] A. Strumia *JHEP* **04** (2011) 073, [arXiv:1101.2195 \[hep-ph\]](#).
- [119] E. Hardy *JHEP* **10** (2013) 133, [arXiv:1306.1534 \[hep-ph\]](#).
- [120] A. Arvanitaki, M. Baryakhtar, X. Huang, K. van Tilburg, and G. Villadoro, *JHEP* **03** (2014) 022, [arXiv:1309.3568 \[hep-ph\]](#).
- [121] M. R. Buckley, D. Feld, S. Macaluso, A. Monteux, and D. Shih, *JHEP* **08** (2017) 115, [arXiv:1610.08059 \[hep-ph\]](#).
- [122] M. Papucci, J. T. Ruderman, and A. Weiler, *JHEP* **09** (2012) 035, [arXiv:1110.6926 \[hep-ph\]](#).
- [123] M. Escudero, A. Berlin, D. Hooper, and M.-X. Lin, *JCAP* **1612** (2016) 029, [arXiv:1609.09079 \[hep-ph\]](#).
- [124] G. F. Giudice and A. Masiero, *Phys. Lett.* **B206** (1988) 480–484.
- [125] G. Bhattacharyya *Phys. Rev.* **D57** (1998) 3944–3949, [arXiv:hep-ph/9707297 \[hep-ph\]](#).
- [126] R. Barbieri and F. Senia, *Eur. Phys. J.* **C75** (2015) no. 12, 602, [arXiv:1506.09201 \[hep-ph\]](#).
- [127] H. Georgi and C. Jarlskog, *Phys. Lett.* **86B** (1979) 297–300.
- [128] R. Barbieri, L. J. Hall, S. Raby, and A. Romanino, *Nucl. Phys.* **B493** (1997) 3–26, [arXiv:hep-ph/9610449 \[hep-ph\]](#).
- [129] B. Bajc and L. Di Luzio, *JHEP* **07** (2015) 123, [arXiv:1502.07968 \[hep-ph\]](#).
- [130] **UTfit**, M. Bona *et al.*, *JHEP* **03** (2008) 049, [arXiv:0707.0636 \[hep-ph\]](#).
- [131] **Heavy Flavor Averaging Group (HFAG)**, Y. Amhis *et al.*, [arXiv:1412.7515 \[hep-ex\]](#).
- [132] **Particle Data Group**, C. Patrignani *et al.*, *Chin. Phys.* **C40** (2016) no. 10, 100001.
- [133] A. Pich *Prog. Part. Nucl. Phys.* **75** (2014) 41–85, [arXiv:1310.7922 \[hep-ph\]](#).
- [134] J. Brod, M. Gorbahn, and E. Stamou, *Phys. Rev.* **D83** (2011) 034030, [arXiv:1009.0947 \[hep-ph\]](#).
- [135] A. Chakraborty and S. Chakraborty, *Phys. Rev.* **D93** (2016) no. 7, 075035, [arXiv:1511.08874 \[hep-ph\]](#).
- [136] F. Feruglio, P. Paradisi, and A. Pattori, [arXiv:1606.00524 \[hep-ph\]](#).

- [137] F. Feruglio, P. Paradisi, and A. Pattori, *JHEP* **09** (2017) 061, [arXiv:1705.00929 \[hep-ph\]](#).
- [138] Y. Kao and T. Takeuchi, [arXiv:0910.4980 \[hep-ph\]](#).
- [139] A. de Gouvea, S. Lola, and K. Tobe, *Phys. Rev.* **D63** (2001) 035004, [arXiv:hep-ph/0008085 \[hep-ph\]](#).
- [140] S. Esch, M. Klasen, D. R. Lamprea, and C. E. Yaguna, *Eur. Phys. J.* **C78** (2018) no. 2, 88, [arXiv:1602.05137 \[hep-ph\]](#).
- [141] B. M. Dassinger, T. Feldmann, T. Mannel, and S. Turczyk, *JHEP* **10** (2007) 039, [arXiv:0707.0988 \[hep-ph\]](#).
- [142] T. Banks, J.-F. Fortin, and S. Thomas, [arXiv:1007.5515 \[hep-ph\]](#).
- [143] **XENON**, E. Aprile *et al.*, *Phys. Rev. Lett.* **121** (2018) no. 11, 111302, [arXiv:1805.12562 \[astro-ph.CO\]](#).
- [144] B. J. Kavanagh, P. Panci, and R. Ziegler, *Submitted to: JHEP* (2018) , [arXiv:1810.00033 \[hep-ph\]](#).
- [145] A. Greljo, J. Martin Camalich, and J. D. Ruiz-Alvarez, *Phys. Rev. Lett.* **122** (2019) no. 13, 131803, [arXiv:1811.07920 \[hep-ph\]](#).
- [146] D. Dercks, H. Dreiner, M. E. Krauss, T. Opferkuch, and A. Reinert, *Eur. Phys. J.* **C77** (2017) no. 12, 856, [arXiv:1706.09418 \[hep-ph\]](#).